BREAST IMAGING

Iran J Radiol. 2019 July; 16(3):e84157. doi: 10.5812/iranjradiol.84157.

Published online 2019 June 3. **Research Article**

Could the "Stiff Rim Sign" Be an Indicator of Lysyl Oxidase Activity in Breast Cancer?

Yasemin Kayadibi [1,*], Fahrettin Kılıç [2], Omer Faruk Karatas [3], Sennur Ilvan [4], Emel Ure Esmerer [5], Turgut Kayadibi [6] and Mehmet Halit Yılmaz [2]

[1]Department of Radiology, Van Training and Research Hospital, Van, Turkey
[2]Department of Radiology, Cerrahpasa Medical Faculty, Istanbul University, Istanbul, Turkey
[3]Department of Molecular Biology and Genetics, Erzurum Technical University, Erzurum, Turkey
[4]Department of Pathology, Cerrahpasa Medical Faculty, Istanbul University, Istanbul, Turkey
[5]Department of Radiology, Hakkari Hospital, Hakkari, Turkey
[6]Department of Plastic Surgery, Van Training and Research Hospital, Van, Turkey

[*]*Corresponding author*: Department of Radiology, Van Training and Research Hospital, Van, Turkey. Email: ysmnkayadibi@gmail.com

Received 2018 September 10; **Revised** 2019 April 07; **Accepted** 2019 April 13.

Abstract

Background: Shear wave elastography (SWE) is a non-invasive and easily applicable imaging modality, which can provide quantitative information of tissue stiffness. Peritumoral high SWE elasticity values (stiff rim sign) has been reported in many studies. Lysyl oxidase (LOX) enzyme is implicated in the formation of peri-tumoral stiffness.
Objectives: The aim of the study was to investigate the correlation between SWE measures with LOX gene expression levels in breast cancer patients.
Patients and Methods: Forty seven women were included in the study. The lesions evaluated by SWE and ultrasound guided tru-cut biopsies were performed from both of the central and peripheral parts. SWE values, LOX family gene expression levels, histopathological features of the lesions, as well as axillary and distant metastasis statuses were evaluated statistically.
Results: Thirty of the patients had breast cancer (BC) (the patient group) and 17 of them had fibroadenoma (the control group). Lysyl oxidase like1 (LOXL1) expression level in BC samples (central parts) were found to be significantly higher than the control group ($P = 0.022$). Stiff rim sign was present in all BC lesions and none of the control group. The elastography values of the patient group were significantly higher than the control group statistically ($P < 0.05$). There was no statistically significant relationship between LOX, LOXL1, LOXL2 expressions and SWE parameters ($P > 0.05$) both for patient and control groups.
Conclusion: Although there were no significant correlations between LOX expressions and SWE parameters in our study, axillary and distant metastasis were found to be correlated with SWE features, which emphasized the prognostic potential of SWE.

Keywords: Breast Cancer, Lysyl Oxidase, Shear Wave Elastography, Genetics

1. Background

The characteristic stiffness of tumors is attributable to collagen crosslinking in the extracellular matrix (ECM) (1, 2). Lysyl oxidase (LOX) is a copper-dependent enzyme catalyzing lysine-dependent crosslink formation in collagen fibers, which is an essential step in collagen fiber formation in ECM (3, 4). The LOX enzyme family consists of LOX enzyme per se and four LOX-like (LOXL1-2-3-4) proteins. Lysyl oxidase, lysyl oxidase like1 (LOXL1), and lysyl oxidase like2 (LOXL2) were found to be associated with breast cancer (BC). LOX was attained maximal levels in front of the area of tumor infiltration and the peripheral fibrotic stroma as pre-metastatic niche formation in the study of Peyrol et al. Increased metastasis and poor prognosis have been shown to be associated with increased LOX expression (5, 6). Patient-specific anti-tumoral biological agents like LOX inhibitors (magnolol and beta-aminopropionitrile) hold promise in the treatment of BC with evolving technology (7).

Shear wave elastography (SWE) is an imaging modality that both reveals and quantifies tissue stiffness (8). It has been reported that elastographic examination shows peritumoral increased stiffness in BC lesions and the "stiff rim sign" is usually used to express these high SWE values measured from peritumoral stroma rather than the tumor itself (8, 9). This phenomenon can be explained by different mechanisms. First, the development of a desmoplastic reaction against tumor cells may serve as the initial defense

against tumor cell infiltration (10, 11). Second, low amplitude (or "noisy") shear waves are attributable to attenuation of sound waves passing through peritumoral tissue (9, 12). Third, peritumoral stiffness may indicate the presence of abnormal tumor-associated collagen fibers and pathological storage thereof in peritumoral tissue (13, 14).

A positive correlation between total fiber collagen area and maximum elasticity determined by SWE has been recently reported in a study of Wang et al. (14). However, up to the present, there was no study about the relationship between SWE and LOX expression levels, which could interpret the SWE values in routine practice.

2. Objectives

Is the peritumoral stiff rim sign that we have detected with SWE an indirect indicator of LOX enzyme activity? If so, SWE could be used in the evaluation of LOX enzyme activity indirectly. In this study, we sought the possible correlation between peritumoral stiff rim sign and LOX enzyme.

3. Patients and Methods

3.1. Patients

This prospective study was approved by the ethics committee of Istanbul University, Cerrahpasa Medical Faculty, and was designed in accordance with the Declaration of Helsinki. Patients' written informed consent forms were obtained before the study. Following the ethical approval, the study was conducted between October 2014 and March 2015. Forty seven women with single breast lesion according to previous sonographic imaging features, who were referred to the radiology department for ultrasound (US) guided core biopsies were included in this study. Patients were divided into two groups according to their histopathological diagnosis. The patients with BC were considered as "patient group". On the other hand, the patients with benign tumoral lesion such as fibroadenoma were considered as the "control group". The current clinical data of the patients including age, lymph node, and distant metastasis were collected from hospital information system after the pathologic diagnoses. Previous breast surgery history, previous diagnosis of breast cancer, chemo or radiotherapy history for any other malignancy and being under age of 18 were our exclusion criteria.

3.2. Imaging Technique

Grayscale ultrasonography (US) and SWE were performed using Aixplorer system (SuperSonic Imagine, Aix-en-Provence, France) equipped with 4 - 15 MHz linear-array transducer. Shear wave velocity colormap was placed over the lesion and while avoiding artifacts, at least one stabilized SWE image for each lesion was acquired by the same single radiologist (YK). A 2 mm circular region of interest (ROI), Q-box, was placed over the stiffest part of the lesion as recommended before (15, 16). Another ROI was placed to the adjacent adipose tissue in the same distance to skin for comparison. Maximum stiffness (Emax), mean stiffness (Emean), SWE-standard deviation (SWE-SD) and lesion-to-fat elasticity ratio (E-ratio) parameters of the lesion were automatically calculated by the system. The presence of a stiff rim sign (higher elasticity from peritumoral tissue than the lesion itself in the range of SWE which was set up at 180 kpa) in the lesions was agreed according to the criteria previously defined by Zhou et al. (9) Final decisions of the SWE features were made with consensus agreement between two radiologists (YK and FK).

3.3. US-Guided Core Biopsy Procedure

After SWE examination, US-guided core biopsy was performed by 14-G biopsy needle (Max-Core®, Bard Biopsy Systems, AZ, USA). The biopsies were performed from the central-tumoral core and peripheral-peritumoral tissue (from the area that corresponds to the hardest part on the SWE images) of the lesions separately. Specimens were collected into Eppendorf tubes, immediately frozen, and kept in -80°C refrigerators until ribonucleotide acid (RNA) extraction for gene expression analysis. In addition, simultaneously taken specimens sent to pathological examination were placed in formalin. Materials were taken from the perilesional area and the center of the lesions, were sent separately to both the genetics and pathology laboratories.

3.4. cDNA Synthesis and Gene Expression Analysis

Total RNA was extracted from equal amounts of tissue materials obtained from participants using "TRIzol" (Invitrogen, United States) reagent in accordance with the manufacturer's instructions. The purities and concentrations of RNA samples were evaluated spectrophotometrically using NanoDrop ND-2000c (Thermo Fisher Scientific, Wilmington, DE). 1000 ng RNA from each sample was reverse transcribed into complementary DNA (cDNA) using "Transcriptor High Fidelity cDNA synthesis kit" (Roche, Switzerland), following the manufacturer's instructions. SYBR Green Master Mix of Roche in a LightCycler480-II real-time thermal cycler (Roche) was used for quantitative reverse-transcription polymerase chain reaction (qRT-PCR). Reactions were performed using the following primer pairs; LOX forward 5'- CGTACGTGCAGAAGATGTCC -3', LOX reverse 5'- AAATCTGAGCAGCACCCTGT -3', LOXL1 forward 5'- GTGTACCGGCCCAACCAG -3', LOXL1 reverse 5'- CTGGCCAGACACTTCTCCTC -3', LOXL2 forward 5'- TGAATATCCAGGTGGAGGACA -3', LOXL2 reverse 5'- CAGGGAAGCCAAACATGC -3'.

The reactions were performed as follows; 1 cycle of 95°C for 5 minutes followed by 40 cycles of 95°C for 10 seconds, 60°C for 20 seconds and 72°C for 25 seconds. LOX, LOXL1, and LOXL2 gene expressions were normalized to ß-actin. Each reaction was performed in duplicate. The relative quantification analysis was done by the d-delta-Ct method, as described previously (17).

3.5. Histopathologic Examination

Specimens were examined for histological type, grade (according to the Scarff-Bloom-Richardson criteria), estrogen receptors (ER), progesterone receptors (PR), human epidermal growth factor receptor-2 (HER-2) expressions in Pathology Department.

3.6. Statistical Analysis

The normality of data was checked before analysis (Kolmogorov-Smirnov) and appropriate tests were selected accordingly. Number cruncher statistical system (NCSS) 2007 software (NCSS, Kaysville, UT, USA) was used for all statistical analyses. We employed either the Mann-Whitney U-test or the Kruskal-Wallis test to seek statistically significant differences between SWE values, histological data, and LOX expression levels. We used Spearman correlation analysis to evaluate relationships among variables. A P value < 0.05 was considered to reflect statistical significance.

4. Results

Thirty lesions were diagnosed as BC (the patient group) and 17 lesions were diagnosed as fibroadenoma (the control group). The histopathological, clinical, and elastographic features of the patients were summarized in Table 1.

Table 1. Sonoelastographic and Histopathological Features of the Lesions[a]

	Measure
Average tumor size, mm	49.57 ± 9.59
SWE values of the patient group (n = 30)	
Average Emean kPa	146.80 ± 49.73
Average SWE-SD	26.12 ± 18.35
SWE values of the control group (n = 17)	
Average Emean kPa	39.06 ± 14.1
Average SWE-SD	2.5 ± 0.5
Histological features of the patient group	
Type of carcinoma	
In-situ ductal carcinoma	2 (6.7)
Tubular carcinoma	1 (3.3)
Invasive ductal carcinoma	24 (80)
Invasive lobular carcinoma	1 (3.3)
Mixed type	2 (6.7)
Grade	
1	1 (3.3)
2	19 (63.3)
3	10 (33.3)
ER (+)	20 (66.7)
PR (+)	17 (56.7)
HER 2 (+)	13 (43.3)
ER (-), **PR** (-), **HER-2** (-)	8 (26)
Axillary node metastasis	17 (56.7)
Distant metastasis	5 (16.7)
Histological features of the control group	
Fibroadenoma	17 (100)

Abbreviations: Emean, mean stiffness; ER, estrogen receptors; HER-2, human epidermal growth factor receptor-2; PR, progesterone receptors; SWE, shear wave elastography; SWE-SD, SWE-standard deviation
[a]Values are expressed as No. (%) unless otherwise indicated.

Stiff rim sign was presented in all BC lesions and none of the control group. The average Emean was 146.80 ± 49.73 kPa from the perilesional hardest area with the stiff rim sign for the patient group and the average Emean was 39.02 ± 14.1 kPa from the central stiffest area for the control group. The elastography values of the patient group were statistically significantly higher than the control group ($P < 0.05$). The mean depth of the lesions was 24.78 ± 13.5 mm. None of our lesions was located deep enough to be affected by rigid structures such as the thoracic wall.

The mean LOXL1 levels were significantly elevated in central parts of the patient group compared to control group samples ($P = 0.022$). Although a slight increase was evident in peripheral parts of the patient group compared to control group samples, this was not significant ($P = 0.136$). No significant difference between central and peripheral materials for both groups was apparent in terms of LOX expression (Figure 1). There was no statistically significant relationship between LOX, LOXL1, LOXL2 expressions and SWE parameters and histopathological findings ($P > 0.05$) both for patient and control groups (Tables 2 and 3). The LOXL2 level correlated significantly with tumor grade. Also, the E-mean value was significantly associated with distant metastasis; as well as the SWE-SD and SWE-ratio with axillary node metastasis (Table 3). Examples of images were shown in Figures 2 and 3.

Table 2. Statistical Analysis of the Correlation Between LOX Expression Levels and SWE[a]

	E mean		E max		SWE-SD		SWE-ratio	
	r	P value	r	P value	r	P value	r	P value
LOX central	-0.116	0.540	-0.199	0.291	0.189	0.318	-0.130	0.494
LOXL1 central	-0.181	0.347	-0.130	0.502	-0.018	0.927	-0.085	0.663
LOXL2 central	-0.012	0.948	0.016	0.934	0.185	0.327	-0.083	0.663
LOX peripheral	0.169	0.390	0.039	0.844	-0.041	0.835	0.089	0.651
LOXL1 peripheral	-0.004	0.985	-0.208	0.289	0.115	0.562	-0.243	0.213
LOXL2 peripheral	0.293	0.123	0.075	0.697	0.282	0.138	-0.254	0.184

Abbreviations: Emean, mean stiffness; Emax, maximum stiffness; E-ratio, lesion-to-fat elasticity ratio; LOX, lysyl oxidase; LOXL, lysyl oxidase-like protein; SWE-SD, shear wave elastography-standard deviation
[a] r, spearman correlation coefficient.

Table 3. P Values of Correlation Analysis Between LOX Expression Levels, SWE Parameters and Histopathological Features of the Patient Group[a]

Parameter	LOX central	LOXL1 central	LOXL2 central	LOX peripheral	LOXL1 peripheral	LOXL2 peripheral	E-mean	E-max	SWE-SD	SWE-ratio
Tumor size	0.523	0.740	0.297	0.838	0.093	0.359	0.853	0.914	0.590	0.826
Tumor grade	0.308	0.076	0.542	0.307	0.463	0.027	0.484	0.946	0.403	0.804
Axillary node metastasis	0.457	0.879	0.869	0.837	0.837	0.650	0.653	0.592	0.014	0.048
Distant metastasis	0.666	0.889	0.706	0.825	0.908	0.978	0.022	0.136	0.208	0.122

Abbreviations: Emean, mean stiffness; Emax, maximum stiffness; SWE-ratio, lesion-to-fat elasticity ratio; LOX, lysyl oxidase; LOXL, lysyl oxidase-like protein; SWE-SD, shear wave elastography-standard deviation
[a] P values for axillary and distant metastases were calculated by Mann Whitney U test; for grade and size, P values were calculated by Spearman's correlation.

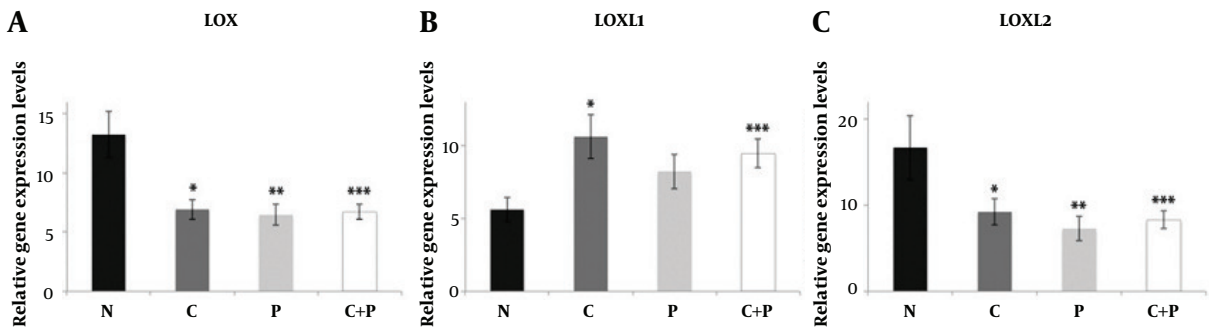

Figure 1. Relative expression levels of LOX (A), LOXL1 (B), and LOXL2 (C) in control and BC patient tissue samples. Data are shown as mean ± standard error of the mean of mRNA levels based on log-transformed values. N: control group, C: samples from central part of the lesions, P: samples from peripheral part of the lesions, C + P: samples from central and peripheral parts together, *P < 0.05; **P < 0.005; ***P < 0.001.(BC, breast cancer; LOX, Lysyl oxidase; LOXL, lysyl oxidase-like).

5. Discussion

In this study, SWE and LOX gene expression values detected in malignant tissues were consistent with the literature and LOXL1 gene expression values were higher in the central regions of the cancerous tissues (9-15). E-max values with distant metastases, SWE ratio and SWE-SD values with axillary metastases were in good correlation. We found no direct correlation between peritumoral elevated elasticity values and LOX gene activity.

Many explanations have been reported in the formation of stiff sign. Peri-tumoral stromal stiffness stemming from abnormal tumor-associated collagen accumulation and lymphangiogenesis has been suggested as the reason for high SWE values measured at the peripheral part of BCs and the amount of collagen was reported to be positively correlated with E-max values (9, 14, 18). Before our study, Hayashi et al. reported a positive correlation be-

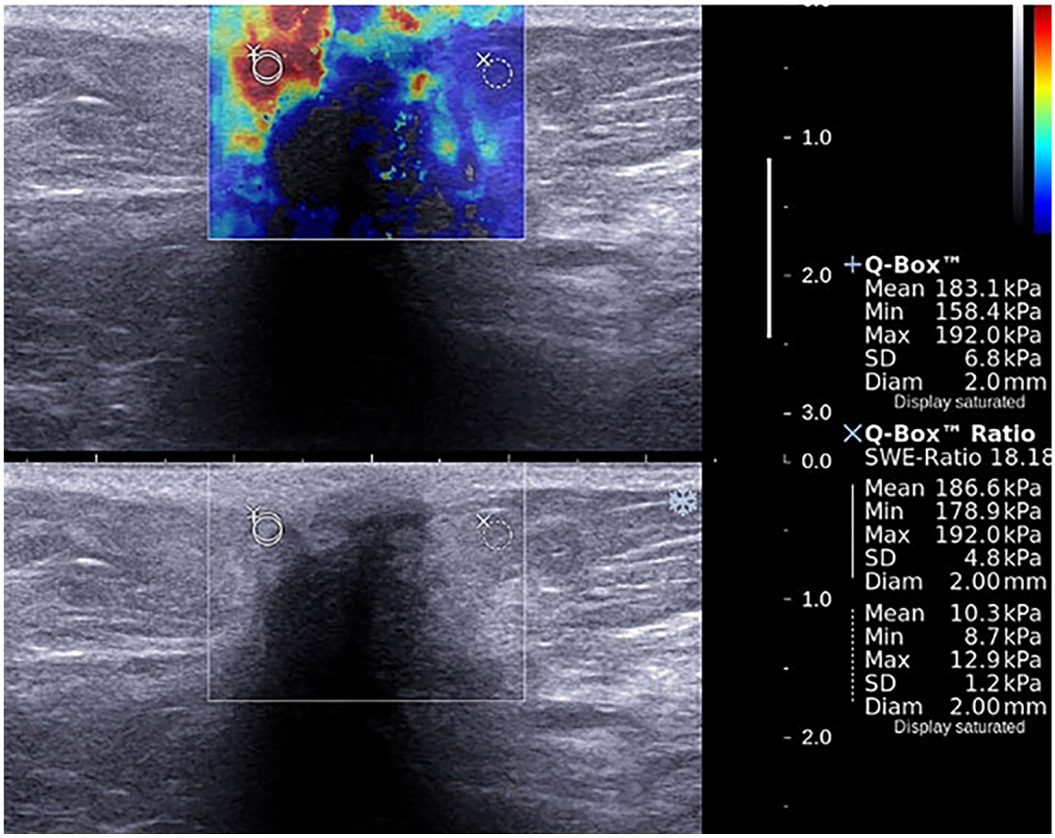

Figure 2. A 40-year-old patient presented with a mass in the upper outer quadrant of the left breast. Shear wave elastography evaluation of the mass showed peritumoral stiffness and central "blind areas". Regions of interest (ROIs) were placed to the stiffest peritumoral area and perilesional fat tissue (Emean = 183 kPa, Emax = 192 kPa). Gray-scale images showed ill defined, hypoechoic mass with acoustic shadow which is suggestive for malignancy. Histopathological diagnosis was grade 2, ER (+), PR (-) and HER-2 (-) invasive ductal carcinoma. Axillary metastasis was negative.

tween strain elastography and the LOX mRNA expression levels of BC lesions. However, in this study, all data were obtained from entire lesions, not from the peripheries. In addition, they studied only BC cases and LOX values of benign breast lesions were not evaluated (19, 20). Actually, the higher LOX activity detected in the central parts of the cancerous tissues in our study is correlated with the findings of Hayashi et al. Our study is the first research that investigates the correlation between SWE features and LOX genes expression levels, which might be considered as a reason for tumor niche formation, and indirectly for the characteristic stiff-rim sign of SWE.

On the other hand, it is known that increased amount of collagen and desmoid reaction are not the only reasons of the highest elasticity values at peripheral parts of BC lesion. Increased precompression by radiologist, reflection of the shear waves by the corners of the lesion, big size, increased inflammation, patient age, depth of the lesion, Doppler flow signal and hard structures beside the lesion as like thoracic wall are other suggested reasons of this increased local stiffness (15, 21, 22).

We have some hypotheses about our results. Firstly, during biopsy, we were careful of obtaining samples from the stiffest points and avoiding precompression but maybe the stiffest points were not the optimal regions of highest LOX expression. Park et al. used multiple ROIs along the stiff rim sign and reported that the stiffness was higher at the borders of the lesion (23). Excisional biopsy instead of core-biopsy and investigation of LOX activity from tumor borders could change the results. Secondly, according to some publications, LOX activity in benign breast lesions and normal parenchyma was found to be higher than that in malignant tissues (24). Not comparing the tumor-bearing and non-tumorous areas of the same patient for LOX activity could be another point that might have affected our results. However, we couldn't get approval from our ethics committee about this point. Thirdly, Peyrol et al. and, Patani et al. suggested that the

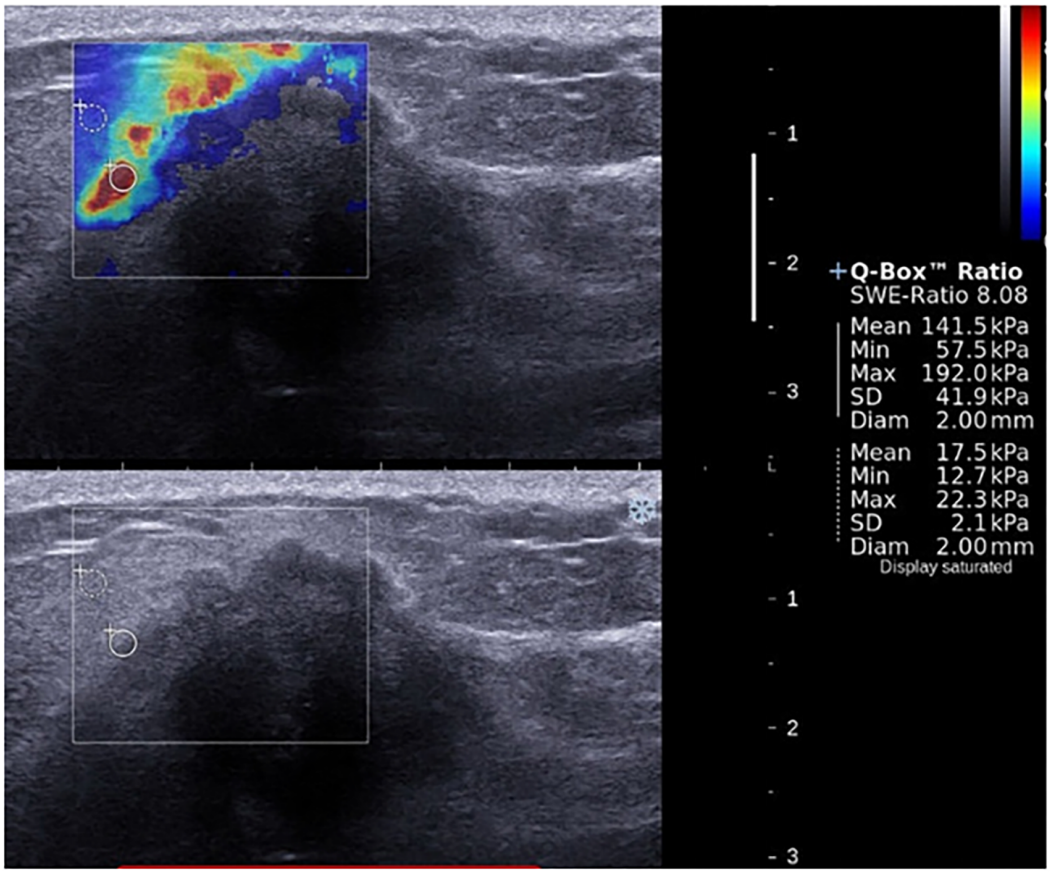

Figure 3. A 39-year-old patient presented with a mass in the upper inner quadrant of the left breast. Shear wave elastography evaluation of the mass showed peritumoral stiffness and central "blind areas". Regions of interest (ROIs) were placed to the stiffest peritumoral area and perilesional fat tissue (Emean = 141 kPa, Emax = 192 kPa). Gray-scale images showed ill defined, hypoechoic mass with acoustic shadow which is suggestive for malignancy. Histopathological diagnosis was grade 2, ER (-), PR (-), and HER-2 (-) invasive lobular carcinoma. Axillary metastasis was positive.

high-level LOX expression in the peritumoral stroma of in-situ ductal carcinoma reflected activation of a host tissue defense (5, 25). As tumor invasion progressed, the LOX expression levels decreased, non-crosslinked collagen deposits increased in number, and the peritumoral stroma became looser. Finally, the tumor overcame the defense mechanism; local invasion triggered angiogenesis and metastasis (5, 25). All but one of the lesions that we studied were invasive and the theory outlined above may explain our finding of high elasticity values associated with low peripheral LOX levels. Both biological and radiological characteristics of peritumoral stroma still remain unclear. Therefore, prospective studies with large number of samples including both in-situ and invasive BC types are needed to point out this relationship in the future.

Chang et al. and Au et al. suggested that tumor size was the most important factor influencing SWE data; larger tumors exhibit a higher-level, peripheral desmoplastic reaction; increased cellularity; and more angiogenesis and edema than do smaller lesions (26, 27). We found no significant correlation between tumor size and any SWE parameter ($P > 0.05$). However, larger tumors tended to have higher Emean values.

Evans et al. had found strong correlations between tumor type (especially invasive lobular carcinoma) and SWE parameters (28) However, the others disagreed about this. Youk et al. and Ganau et al. found no significant difference in any SWE parameter by the type of lobular cancer studied (29, 30). However, Brkljacic et al. found that invasive lobular carcinomas were stiffer than invasive ductal carcinomas < 1.5 cm in diameter (31). The pathological diagnoses of our patients were: 6.7% (n = 2) ductal carcinoma in situ, 3.3% (n = 1) tubular carcinoma, 80.0% (n = 24) invasive ductal carcinoma, 3.3% (n = 1) invasive lobular carcinoma, and 6.7% (n = 2) mixed. Most lesions were invasive ductal carcinomas; thus, we could not seek correlations between SWE

data and histological type.

In our study, we found that patients with axillary metastases have significantly higher SWE-ratio values (P = 0.048) and SWE-SD (0.014). Also, Emean values were significantly higher (P = 0.022) with distant metastases (liver, bone, and/or cranial metastases) compared to the patients with no-metastases.

Our study had several limitations. Although we did not look for inter- and intra-observer reliability in our study, previous studies have shown that reproducibility of SWE technique is high (9, 32). The work was performed in a single center and our patient number was small. The number of lesions we could examine was limited. We did not compare the depths of the lesions. Therefore, prospective studies with larger numbers of both in-situ and invasive BCs are needed.

In conclusion, stiff rim sign is a feature that enhances the diagnostic and prognostic properties of SWE and in our study, we evaluated LOX values with stiff rim sign for the first time. The results of this study showed that, a statistically significant correlation between SWE parameters and LOX, LOXL-1 and LOXL-2 expression might not be present. Prospective studies with a large number of patients and large lesion profiles including in-situ lesions and different histopathological subtypes are needed to be conducted in the future to validate this relationship.

Footnotes

Authors' Contributions: Study concept and design: Yasemin Kayadibi; acquisition of data: Yasemin Kayadibi, Omer Faruk Karatas, Fahrettin Kılıç, and Turgut Kayadibi; analysis and interpretation of data: Omer Faruk Karatas; drafting of the manuscript: Yasemin Kayadibi; critical revision of the manuscript for important intellectual content: Mehmet Halit Yılmaz; statistical analysis: Emel Ure Esmerer; administrative, technical, and material support: Omer Faruk Karatas, Sennur Ilvan; study supervision: Yasemin Kayadibi

Conflict of Interests: None declared.

Ethical Considerations: 83045809/18220.

Financial Disclosure: There are no financial conflicts of interest to disclose.

Funding/Support: This research was funded by Cerrahpasa Medical Faculty by grant No.: 83045809-18220.

References

1. Helleman J, Jansen MP, Ruigrok-Ritstier K, van Staveren IL, Look MP, Meijer-van Gelder ME, et al. Association of an extracellular matrix gene cluster with breast cancer prognosis and endocrine therapy response. *Clin Cancer Res*. 2008;**14**(17):5555–64. doi: 10.1158/1078-0432.CCR-08-0555. [PubMed: 18765548].
2. Tilghman RW, Cowan CR, Mih JD, Koryakina Y, Gioeli D, Slack-Davis JK, et al. Matrix rigidity regulates cancer cell growth and cellular phenotype. *PLoS One*. 2010;**5**(9). e12905. doi: 10.1371/journal.pone.0012905. [PubMed: 20886123]. [PubMed Central: PMC2944843].
3. Smith-Mungo LI, Kagan HM. Lysyl oxidase: Properties, regulation and multiple functions in biology. *Matrix Biol*. 1998;**16**(7):387–98. doi: 10.1016/S0945-053X(98)90012-9. [PubMed: 9524359].
4. Nishioka T, Eustace A, West C. Lysyl oxidase: From basic science to future cancer treatment. *Cell Struct Funct*. 2012;**37**(1):75–80. doi: 10.1247/csf.11015. [PubMed: 22453058].
5. Peyrol S, Raccurt M, Gerard F, Gleyzal C, Grimaud JA, Sommer P. Lysyl oxidase gene expression in the stromal reaction to in situ and invasive ductal breast carcinoma. *Am J Pathol*. 1997;**150**(2):497–507. [PubMed: 9033266]. [PubMed Central: PMC1858268].
6. Decitre M, Gleyzal C, Raccurt M, Peyrol S, Aubert-Foucher E, Csiszar K, et al. Lysyl oxidase-like protein localizes to sites of de novo fibrinogenesis in fibrosis and in the early stromal reaction of ductal breast carcinomas. *Lab Invest*. 1998;**78**(2):143–51. [PubMed: 9484712].
7. Bondareva A, Downey CM, Ayres F, Liu W, Boyd SK, Hallgrimsson B, et al. The lysyl oxidase inhibitor, beta-aminopropionitrile, diminishes the metastatic colonization potential of circulating breast cancer cells. *PLoS One*. 2009;**4**(5). e5620. doi: 10.1371/journal.pone.0005620. [PubMed: 19440335]. [PubMed Central: PMC2680032].
8. Barr RG. *Breast elastograph*. New York: Thieme Publishers; 2015. doi: 10.1055/b-0035-121483.
9. Zhou J, Zhan W, Chang C, Zhang X, Jia Y, Dong Y, et al. Breast lesions: Evaluation with shear wave elastography, with special emphasis on the "stiff rim" sign. *Radiology*. 2014;**272**(1):63–72. doi: 10.1148/radiol.14130818. [PubMed: 24661245].
10. Itoh A, Ueno E, Tohno E, Kamma H, Takahashi H, Shiina T, et al. Breast disease: Clinical application of US elastography for diagnosis. *Radiology*. 2006;**239**(2):341–50. doi: 10.1148/radiol.2391041676. [PubMed: 16484352].
11. Liu B, Zheng Y, Huang G, Lin M, Shan Q, Lu Y, et al. Breast lesions: Quantitative diagnosis using ultrasound shear wave elastography-A systematic review and meta-analysis. *Ultrasound Med Biol*. 2016;**42**(4):835–47. doi: 10.1016/j.ultrasmedbio.2015.10.024. [PubMed: 26778289].
12. Barr RG. Shear wave imaging of the breast: Still on the learning curve. *J Ultrasound Med*. 2012;**31**(3):347–50. doi: 10.7863/jum.2012.31.3.347. [PubMed: 22368124].
13. Evans A, Rauchhaus P, Whelehan P, Thomson K, Purdie CA, Jordan LB, et al. Does shear wave ultrasound independently predict axillary lymph node metastasis in women with invasive breast cancer? *Breast Cancer Res Treat*. 2014;**143**(1):153–7. doi: 10.1007/s10549-013-2747-z. [PubMed: 24305976]. [PubMed Central: PMC4363519].
14. Wang ZL, Sun L, Li Y, Li N. Relationship between elasticity and collagen fiber content in breast disease: A preliminary report. *Ultrasonics*. 2015;**57**:44–9. doi: 10.1016/j.ultras.2014.10.016. [PubMed: 25465961].
15. Barr RG, Zhang Z. Effects of precompression on elasticity imaging of the breast: Development of a clinically useful semiquantitative method of precompression assessment. *J Ultrasound Med*. 2012;**31**(6):895–902. doi: 10.7863/jum.2012.31.6.895. [PubMed: 22644686].
16. Skerl K, Vinnicombe S, Giannotti E, Thomson K, Evans A. Influence of region of interest size and ultrasound lesion size on the performance of 2D shear wave elastography (SWE) in solid breast masses. *Clin Radiol*. 2015;**70**(12):1421–7. doi: 10.1016/j.crad.2015.08.010. [PubMed: 26455652].
17. Livak KJ, Schmittgen TD. Analysis of relative gene expression data using real-time quantitative PCR and the 2(-delta delta C(T)) method. *Methods*. 2001;**25**(4):402–8. doi: 10.1006/meth.2001.1262. [PubMed: 11846609].

18. Tozaki M, Fukuma E. Pattern classification of shear wave elastography images for differential diagnosis between benign and malignant solid breast masses. *Acta Radiol*. 2011;**52**(10):1069–75. doi: 10.1258/ar.2011.110276. [PubMed: 22013011].
19. Hayashi M, Yamamoto Y, Ibusuki M, Fujiwara S, Yamamoto S, Tomita S, et al. Evaluation of tumor stiffness by elastography is predictive for pathologic complete response to neoadjuvant chemotherapy in patients with breast cancer. *Ann Surg Oncol*. 2012;**19**(9):3042–9. doi: 10.1245/s10434-012-2343-1. [PubMed: 22476757].
20. Hayashi M, Yamamoto Y, Sueta A, Tomiguchi M, Yamamoto-Ibusuki M, Kawasoe T, et al. Associations between elastography findings and clinicopathological factors in breast cancer. *Medicine (Baltimore)*. 2015;**94**(50). e2290. doi: 10.1097/MD.0000000000002290. [PubMed: 26683963]. [PubMed Central: PMC5058935].
21. Xiao Y, Yu Y, Niu L, Qian M, Deng Z, Qiu W, et al. Quantitative evaluation of peripheral tissue elasticity for ultrasound-detected breast lesions. *Clin Radiol*. 2016;**71**(9):896–904. doi: 10.1016/j.crad.2016.06.104. [PubMed: 27349474].
22. Xiang L, Ma F, Yao M, Xu G, Pu H, Liu H, et al. Benign lesion evaluation: Factors causing the "stiff rim" sign in breast tissues using shear-wave elastography. *Br J Radiol*. 2019;**92**(1094):20180602. doi: 10.1259/bjr.20180602. [PubMed: 30303694]. [PubMed Central: PMC6404811].
23. Park HS, Shin HJ, Shin KC, Cha JH, Chae EY, Choi WJ, et al. Comparison of peritumoral stromal tissue stiffness obtained by shear wave elastography between benign and malignant breast lesions. *Acta Radiol*. 2018;**59**(10):1168–75. doi: 10.1177/0284185117753728. [PubMed: 29359949].
24. Chen LC, Tu SH, Huang CS, Chen CS, Ho CT, Lin HW, et al. Human breast cancer cell metastasis is attenuated by lysyl oxidase inhibitors through down-regulation of focal adhesion kinase and the paxillin-signaling pathway. *Breast Cancer Res Treat*. 2012;**134**(3):989–1004. doi: 10.1007/s10549-012-1986-8. [PubMed: 22434522].
25. Patani N, Jiang W, Newbold R, Mokbel K. Prognostic implications of carboxyl-terminus of Hsc70 interacting protein and lysyl-oxidase expression in human breast cancer. *J Carcinog*. 2010;**9**:9. doi: 10.4103/1477-3163.72505. [PubMed: 21139993]. [PubMed Central: PMC2997236].
26. Chang JM, Moon WK, Cho N, Kim SJ. Breast mass evaluation: Factors influencing the quality of US elastography. *Radiology*. 2011;**259**(1):59–64. doi: 10.1148/radiol.10101414. [PubMed: 21330569].
27. Au FW, Ghai S, Lu FI, Moshonov H, Crystal P. Quantitative shear wave elastography: Correlation with prognostic histologic features and immunohistochemical biomarkers of breast cancer. *Acad Radiol*. 2015;**22**(3):269–77. doi: 10.1016/j.acra.2014.10.007. [PubMed: 25666048].
28. Evans A, Whelehan P, Thomson K, McLean D, Brauer K, Purdie C, et al. Invasive breast cancer: Relationship between shear-wave elastographic findings and histologic prognostic factors. *Radiology*. 2012;**263**(3):673–7. doi: 10.1148/radiol.12111317. [PubMed: 22523322].
29. Youk JH, Gweon HM, Son EJ, Kim JA, Jeong J. Shear-wave elastography of invasive breast cancer: Correlation between quantitative mean elasticity value and immunohistochemical profile. *Breast Cancer Res Treat*. 2013;**138**(1):119–26. doi: 10.1007/s10549-013-2407-3. [PubMed: 23324903].
30. Ganau S, Andreu FJ, Escribano F, Martin A, Tortajada L, Villajos M, et al. Shear-wave elastography and immunohistochemical profiles in invasive breast cancer: Evaluation of maximum and mean elasticity values. *Eur J Radiol*. 2015;**84**(4):617–22. doi: 10.1016/j.ejrad.2014.12.020. [PubMed: 25619502].
31. Brkljacic B, Divjak E, Tomasovic-Loncaric C, Tesic V, Ivanac G. Shear-wave sonoelastographic features of invasive lobular breast cancers. *Croat Med J*. 2016;**57**(1):42–50. doi: 10.3325/cmj.2016.57.42. [PubMed: 26935613]. [PubMed Central: PMC4800323].
32. Evans A, Whelehan P, Thomson K, Brauer K, Jordan L, Purdie C, et al. Differentiating benign from malignant solid breast masses: value of shear wave elastography according to lesion stiffness combined with greyscale ultrasound according to BI-RADS classification. *Br J Cancer*. 2012;**107**(2):224–9. doi: 10.1038/bjc.2012.253. [PubMed: 22691969]. [PubMed Central: PMC3394981].